The European Research Journal 2024;10(5):522-532 Original Article

DOI: https://doi.org/10.18621/eurj.1518743 *Bioengineering*

Impact of internal phase volume on the physical, morphological and mechanical characteristics of emulsion templated scaffolds

Betül Aldemir Dikici

Department of Bioengineering, Faculty of Engineering, Izmir Institute of Technology, İzmir, Türkiye

ABSTRACT

Objectives: The high porosity of tissue engineering scaffolds is advantageous as they provide a high degree of infiltration of nutrients, enable cell penetration, and support vascularisation. However, the mechanical strength is also critical for providing structural support to the defect site throughout the regeneration process. In this study, we aimed to establish a relationship between internal phase volume and emulsion-templated scaffolds' physical, morphological and mechanical characteristics.

Methods: In this work, tetra methacrylate functionalised polycaprolactone (4PCLMA) polymers were synthesised via ring-opening polymerisation followed by methacrylation. 4PCLMA-based emulsion templated matrices with 60%, 75% and 82% internal phase volumes were fabricated (P60, P75, and P82). These scaffolds' densities, porosities, average pore and window sizes, degree of interconnectivity values, and mechanical properties were investigated.

Results: Increasing internal phase volume reduced the density of the foams by almost two-fold. No direct correlation was observed between average pore size and internal phase volume. Both the average window sizes and the degree of interconnectivity values increase with increasing internal phase volume. Compression modulus values are calculated as 0.46±0.04 MPa, 0.23±0.02 MPa and 0.14±0.01 MPa for P60, P75, and P82, respectively. Increasing internal phase volume from 60% to 82% caused a more than 2-fold reduction in the stiffness of the emulsion-templated matrices.

Conclusions: Accordingly, by reporting on this experimental framework, we established a relationship between internal phase volume and the physical, morphological and mechanical characteristics of 4PCMA-based scaffolds to precisely engineer these characteristics for specific tissue engineering applications.

Keywords: Biomaterials, emulsion templating, porosity, tissue engineering, mechanical characterisation

Polymer foams are cellular polymeric materials that have a wide range of applications, such as thermal energy storage [1], sound insulation [2], filtration and separation, packaging, battery applications [3], environmental applications [4-6] and biomedical applications [7-10]. In the biomedical field, one of the most popular applications of polymeric foams is their use as 3D cell culture platforms or tissue engineering scaffolds [11, 12]. Tissue engineering is a multidisciplinary field that combines the principles of

Corresponding author: Betül Aldemir Dikici, PhD., Assist. Prof.
Phone: +90 232 750 60 00, E-mail: aldemirbetul@gmail.com

How to cite this article: Aldemir Dikici B. Impact of internal phase volume on the physical, morphological and mechanical characteristics of emulsion templated scaffolds. Eur Res J. 2024;10(5):522-532. doi: 10.18621/eurj.1518743

Received: July 18, 2024
Accepted: August 23, 2024
Published Online: August 27, 2024

biology and engineering and looks for solutions for the regeneration of tissues [13]. In scaffold-based tissue engineering, 3D porous matrices (scaffolds) are implanted into the defect site and provide a surface for cell attachment, proliferation and mechanical support until the tissue is regenerated. There are various scaffold fabrication techniques, such as electrospinning, decellularisation [14], freeze-drying [15], porogen leaching [16, 17], and 3D printing [18].

Emulsion templating is another porous polymer fabrication route with a vast number of advantages [2, 19-22]. In this technique, an emulsion is created using two immiscible liquids where the droplets are defined as the internal phase, and the liquid that covers the internal phase is defined as the continuous phase. Polymers/polymer solutions form the continuous phase, and depending on the polymer properties, both water-in-oil (w/o) and oil-in-water (o/w) emulsions can be used. Surfactants [23-26] or Pickering particles [27] are used to provide emulsion stability by reducing the surface tension and providing a mechanical barrier between the two phases, respectively. Depending on the nature of the polymer, the continuous phase of the emulsion is polymerised either by thermal or photo polymerisation or solvent evaporation. Once the polymer is solidified, water droplets in the internal phase are removed, and the porous matrices are obtained (Fig. 1) [7].

If the volume of the internal phase in the emulsion is more than 74%, these emulsions are classified as High Internal Phase Emulsions (HIPE). Emulsions with an internal phase volume of 30-74% are defined as Medium Internal Phase Emulsions (MIPE). The matrices obtained with their polymerisation are named PolyHIPEs and PolyMIPEs, respectively [28]. Porous materials can have open cellular and closed cellular morphologies. Open cellular structures are characterised by the presence of windows that connect neighbouring pores to each other (Fig. 2). PolyHIPEs and PolyMIPEs generally exhibit open-cellular structures due to the high packing density of the water droplets. Polymer film between droplets gets thin and ruptures during polymerisation, resulting in the formation of windows [19].

In the design of tissue engineering scaffolds, high porosity with high interconnectivity (open cellular architecture) is desired to provide a high degree of infiltration of nutrients, enable cell penetration, and support vascularisation. However, the mechanical strength of a material is also critical for providing structural support to the defect site throughout the regeneration process [29].

One other advantage of emulsion-templated matrices is the high tunability of their morphology and, correspondingly, their mechanical properties [7, 24, 30]. Both emulsion formulation and the process parameters, such as temperature and stirring speed [31], have a direct impact on the morphological characteristics of the scaffolds. Oil and water phase components [32, 33], their amounts, and the relative ratios of their sub-components [23] have a direct impact on architectural features and mechanical properties. As the internal phase volume defines the porosity of the emulsion-templated matrices, scaffolds with a high degree of porosity could be easily obtained simply by increasing the water content of the emulsion.

This study aims to investigate the impact of internal phase volume on the physical, morphological, and mechanical characteristics of photocurable polycaprolactone (PCL) based emulsion templated scaffolds.

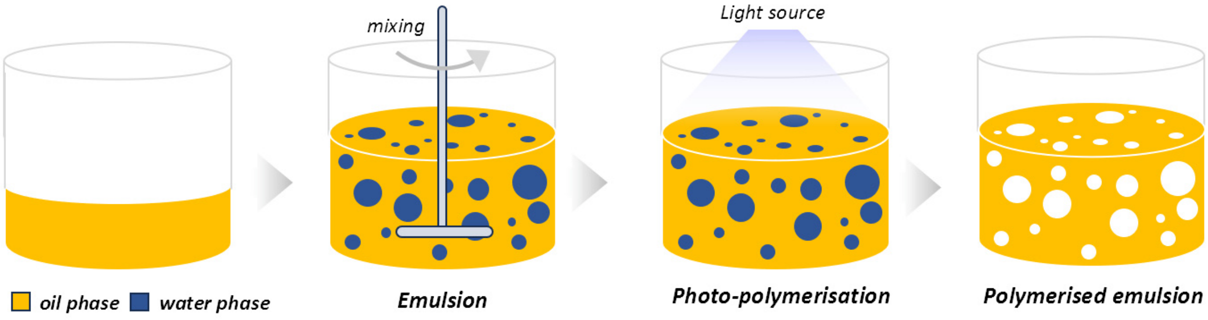

Fig. 1. **Fabrication steps of emulsion templated matrices.**

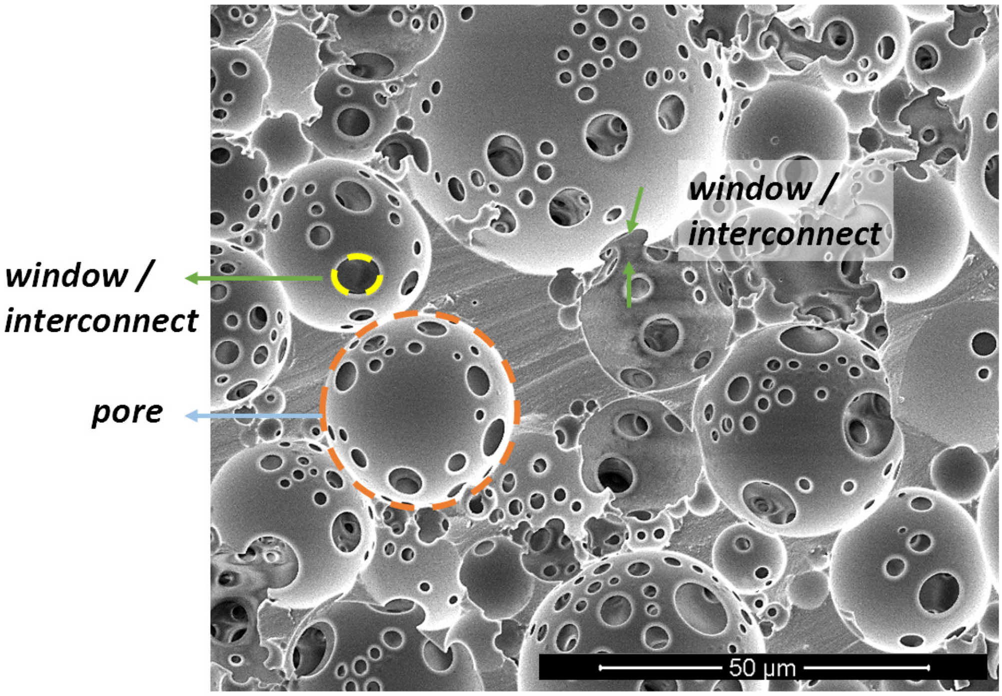

Fig. 2. **Scanning electron microscope micrograph of a scaffold fabricated via emulsion templating (an orange circle and blue arrow indicate pores, and a yellow circle or green arrow indicates windows/interconnects).**

PCL is a biocompatible and bioresorbable polymer and one of the most advantageous biomaterials for use in the biomedical field [34]. Accordingly, in this work, tetra methacrylate functionalised polycaprolactone (4PCLMA) polymers were synthesised via ring-opening polymerisation followed by methacrylation. 4PCLMA-based emulsion templated matrices with internal phase volumes of 60%, 75% and 82% were fabricated. Densities, porosities, morphologies, average pore and window sizes, pore and window size distributions, degree of interconnectivity values and mechanical properties of these scaffolds were investigated, and the changes in these parameters in relation to internal phase volume were discussed.

METHODS

Polyglycerol polyricinoleate (PGPR) was used as a surfactant in the emulsion composition and was kindly donated by Paalsgard (Juelsminde, Denmark). Ɛ-caprolactone, pentaerythritol, tin (II) 2-ethylhexanoate, dichloromethane (DCM), and triethylamine (TEA), methacrylic anhydride (MAAn), hydrochloric acid (HCl), photoinitiator (2,4,6-trimethylbenzoyl phosphine oxide/2-hydroxy-2-methylpropiophenone blend) and dichloroethane (DCE) were purchased from Sigma Aldrich and used without further modifications unless otherwise stated.

Polymer Synthesis

A detailed protocol for the synthesis of photocurable PCL has been described elsewhere (Fig. 3) [35, 36]. Briefly, Ɛ-caprolactone and pentaerythritol were mixed at 160°C in a flask until pentaerythritol was dissolved. Then, tin (II) 2-ethylhexanoate was added as a catalyst, and the system was left for the reaction overnight. At the end of the synthesis of the hydroxyl-terminated polymer, the system was cooled down to room temperature. The obtained 4PCL was dissolved in DCM, and TEA was added. Then, the flask was transferred to an ice bath. In a separate beaker, MAAn was dissolved in DCM, the solution was added via a dropping funnel and all the setup was kept for the reaction at room temperature for 68 hours. Then, 4PCLMA was washed with hydrochloric acid (HCl) solution and deionised water, respectively, and the solvent was removed using a rotary evaporator. Finally,

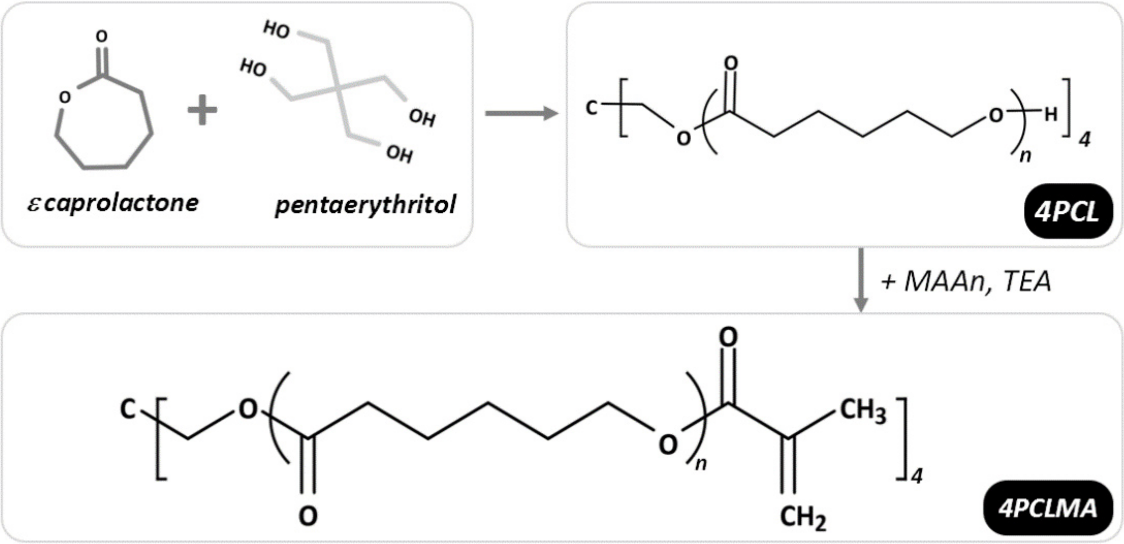

Fig. 3. Synthesis and methacrylation of 4-arm PCL.

the polymer was washed with methanol, and the solvent was removed. The resulting 4PCLMA was stored for further use.

Synthesis of MIPEs and HIPEs and Their Polymerization

Three compositions of emulsions with varying internal phase volumes were prepared: 60%, 75% and 82% for P60, P75 and P82, respectively. The amounts of the ingredients of each component of the emulsion are given in Table 1. Briefly, 4PCLMA, surfactant (PGPR), photoinitiator and solvent (DCE) were mixed using a magnetic stirrer at 370 rpm in a glass container for 1 minute to create a homogeneous blend. Then, water as an internal phase was added dropwise using a Pasteur pipette to the mixture. Lastly, the emulsion was mixed for 2 minutes, transferred into circular silicone moulds with a diameter of 6 mm and height of 4 mm, respectively, and photocured for 2 minutes on each side. All emulsion compositions were cured immediately (within 10 s) once prepared. The obtained MIPEs and HIPEs were washed with methanol to remove any remaining contaminants of uncured polymer, surfactant, or solvent, and the scaffolds were freeze-dried.

Densities of Emulsion Templated Matrices

The densities of polymerised emulsions were calculated by measuring the mass (m) and volume (V) values of the cylindrical samples (Equation 1) [37].

$$density = \frac{m}{V} = \frac{m}{\pi r^2 h} \tag{1}$$

Porosities of Emulsion Templated Matrices

Equation 2 was used to calculate the porosities of the polymerised emulsions [35, 36].

$$\%\,Porosity = (1 - \frac{\rho_{PolyHIPE}}{\rho_{wall}}) \times 100 \tag{2}$$

$\rho_{PolyHIPE}$ and ρ_{wall} state the densities of PolyHIPE and the wall of the PolyHIPE, respectively. The wall density is the measured density of the bulk polymer.

Morphological Characterization

Scanning electron microscopy (SEM) was used to investigate the morphology of the fabricated scaffolds. Cross-sectional samples were prepared from dried polymerised emulsions, and all samples were placed on aluminium pins coated with carbon stickers. Then, samples were gold coated and visualised using SEM (FEI QUANTA 250 FEG, United States).

Pore and Window Size Quantification

100 pores and 150 windows were selected randomly from three different regions of the samples, and measurements were taken using Image J [38]. A sta-

Table 1. Ingredients of the emulsions and characteristics of the polymerised emulsions

	P60	P75	P82
4PCLMA (g)	0.2	0.2	0.2
PGPR (g)	0.03	0.03	0.03
DCE (g)	0.53	0.53	0.53
PI (g)	0.03	0.03	0.03
Water (mL)	1	2	3
Internal phase (%)	60	75	82
Density (g/cm^3)	0.395	0.258	0.208
Porosity (%)	65±1	77±1	81±2
Pore size (D, µm)	45±21	38±17	50±26
Window size (d, µm)	4±4	5±3	9±4
Degree of interconnectivity (d/D)	0.089	0.132	0.180
Compression modulus (MPa)	0.46±0.04	0.23±0.02	0.14±0.01

4PCLMA= tetra methacrylate functionalized polycaprolactone, PGPR=Polyglycerol polyricinoleate, DCE=dichloroethane, PI=photoinitiator, MPa= Megapascal

tistical correction factor (2/√3) was applied for the measured pore values to correct the underestimation of the measurements due to uneven sectioning [7, 26]. Pore and window histograms were created using Microsoft Excel. The degree of interconnectivity values were calculated by dividing the average window diameter by the average pore diameter (d/D) [7].

Compression Test

Mechanical characterisation of 4PCLMA-based emulsion templated matrices was conducted using a compact tabletop universal tester with a 100 N load cell (EZ-TEST EZ-S, Shimadzu, Japan). Cylindrical discs with approximately 5.5 mm diameter and 3.5 mm height were used. The exact dimensions of the samples were measured using a calipper, and recorded. Compression samples were placed on the bottom part of the compression plate, the upper place was lowered, and the compressive tests were performed at the rate of 1 mm/min. Samples were compressed up to 90 N or until ~70% strain was achieved. The compression modulus values were calculated from the linear region of the stress-strain curve of each sample [39].

Statistical Analysis

GraphPad Prism 6 was used to perform statistical analyses. One-way analysis of variance (ANOVA) was applied for mechanical testing, and the graph was plotted as mean ± SD. A difference was deemed statistically significant if the P-value was less than 0.05, and the statistical differences are denoted in the figures. The total number of replicates (n) is stated in the figure legends, where relevant.

RESULTS

Fabrication of PCL PolyMIPEs and PolyHIPEs

Following polymer synthesis, all three groups of emulsion-templated scaffolds were successfully fabricated. There was no observable phase separation during and right after emulsification until the photopolymerisation. 60%, 75% and 82% water were incorporated into the emulsion composition as an internal phase for groups P60, P75 and P82, respectively.

At the end of the emulsification and mixing process, all three groups formed opaque and white emulsions but with different observable viscosities. Whilst P60 has the lowest observable viscosity among these three groups, and the emulsion was transferred into the moulds by pouring, P75 was comparably more viscous. Accordingly, increasing the internal phase volume to 82% increased the observable viscosity of the emulsion, and P82 has a mayonnaise-like consistency and could not be transferred into the mould by pouring; it was transferred using a spatula. Following the polymerisation of the emulsions, they were fully solidified, and no visible uncured region was detected when samples were cross-sectioned using a surgical blade.

Impact of Internal Phase Volume on the Physical and Morphological Characteristics of Emulsion Templated Scaffolds

Densities of emulsion-templated scaffolds were measured as 0.395, 0.258 and 0.208 g/cm3 for P60, P75 and P82, respectively. Increasing internal phase volume reduced the density of the foams. Porosities were measured as 65%, 77% and 81% for emulsions, with internal phase volumes of 60%, 75%, and 82%.

Following polymerisation and post-washing processes, scaffolds were freeze-dried to prevent any potential collapse, which was morphologically investigated by SEM. Fig. 4 shows the morphologies of P60, P75 and P82 at three different magnifications. At this point, it is critical to distinguish the difference between the polydisperse distribution of the pores and heterogeneous morphology. The polydisperse distribution of the pores indicates the broad distribution of the pore sizes. However, if this polydisperse distribution is in a similar trend throughout the sample, it can be concluded that these samples have homogenous morphology. Capturing multiple images from different regions of the samples and having a zoom-out image that shows the morphology of the full thickness of the sample can give an idea of these two characteristics. As shown in the first column (Figs. 4A, 4D and 4G), polydisperse pores are homogeneously dispersed throughout the scaffolds in all three groups of scaffolds. There is no heterogeneous region different from the overall morphology. Also, no separated full layer of non-porous polymer phase was detected.

The average pore sizes were measured as 45±21 µm, 38±17 µm, and 50±26 µm for P60, P75, and P82, respectively. When the internal phase volume was increased to 82%, water droplets incorporated into the emulsion composition took a longer time to melt in the emulsion during the emulsification process. It is an indication that 82% is around the maximum internal phase volume that could be incorporated into the emulsion composition. Thus, although the frequency

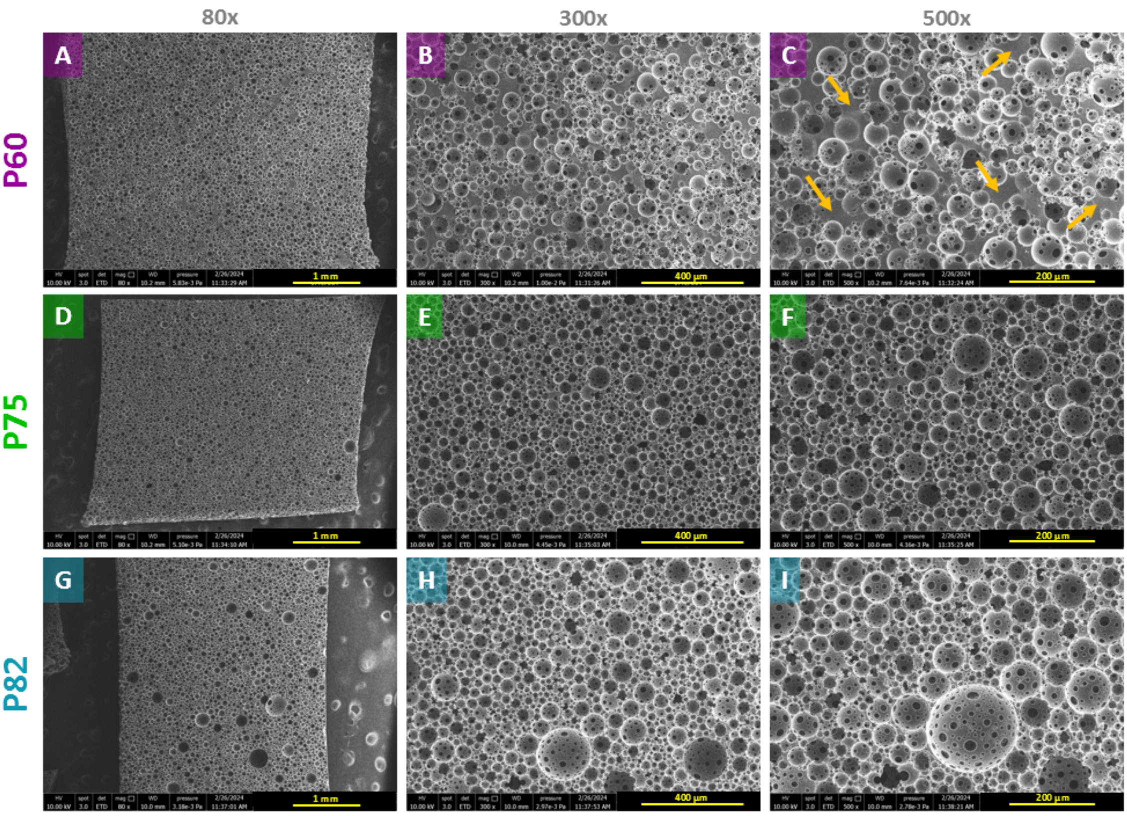

Fig. 4. **Scanning electron microscope images of polymerised emulsions prepared with varying internal phase volumes. (A-C) P60, (D-F) P75, and (G-I) P82. Orange arrows indicate non-porous regions.**

of pores with pore sizes between 30-40 µm is around 20-50% in both P75 and P82, the frequency of pores with pore sizes larger than 70 µm is 11% and 27%, respectively (Figs. 5B and 5C). Pore and window size distributions become broader in P82 when compared with P60 and P75 (Figs. 5A-5F).

The average window sizes were measured as 4±4 µm, 5±3 µm, and 9±4 µm, and the degree of interconnectivity values were calculated as 0.089, 0.132, and 0.180 for P60, P75, and P82, respectively. Both the average window sizes and the degree of interconnectivity values increased with increasing internal phase volume.

Impact of Internal Phase Volume on the Mechanical Characteristics of Emulsion Templated Scaffolds

Cylindrical samples were prepared, and the compression test was conducted to investigate the impact of internal phase volume on the mechanical characteristics of emulsion-templated scaffolds. None of the samples undergo failure under this condition. Compressive stress−strain curves of polymerised emulsions and their compressive modulus calculated from the linear region of the stress-strain curve are given in Figs. 6A and 6B, respectively.

A significant difference can be seen in stress-strain curves of emulsion-templated matrices fabricated with varying internal phase volumes (Fig. 6A). At low strain, where stiffness values were calculated, stress-strain values were linear, and dramatic increases in stress were observed with increasing strain. Compression modulus values are calculated as 0.46±0.04 MPa, 0.23±0.02 MPa and 0.14±0.01 MPa for P60, P75, and P82, respectively.

DISCUSSION

The densities of the foams were observed to reduce when internal phase volume increased, as increasing water content resulted in a reduction in the amount of solid materials per unit volume [7, 40].

Porosity values were calculated close to but not the same as internal phase volumes. Although the internal phase is the ingredient responsible for the formation of the pores and, consequently, the porosity, the difference between internal phase volume and the porosity of the emulsion-templated matrices has been reported before [35]. Some of the potential reasons be-

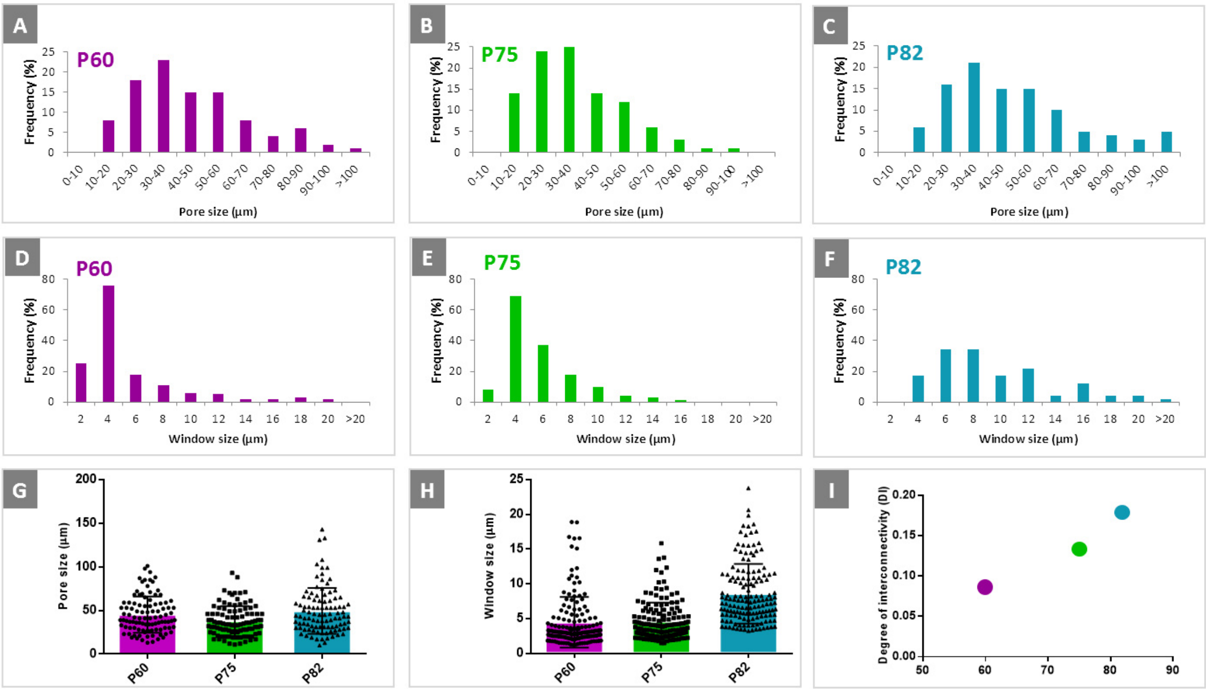

Fig. 5. **Morphological characterisation of polymerised emulsions: (A-C) pore size distribution histograms, (D-F) window size distribution histograms, (G) average pore size, (H) average window size and (I) degree of interconnectivity graphs of polymerised emulsions (P60, P75 and P82).**

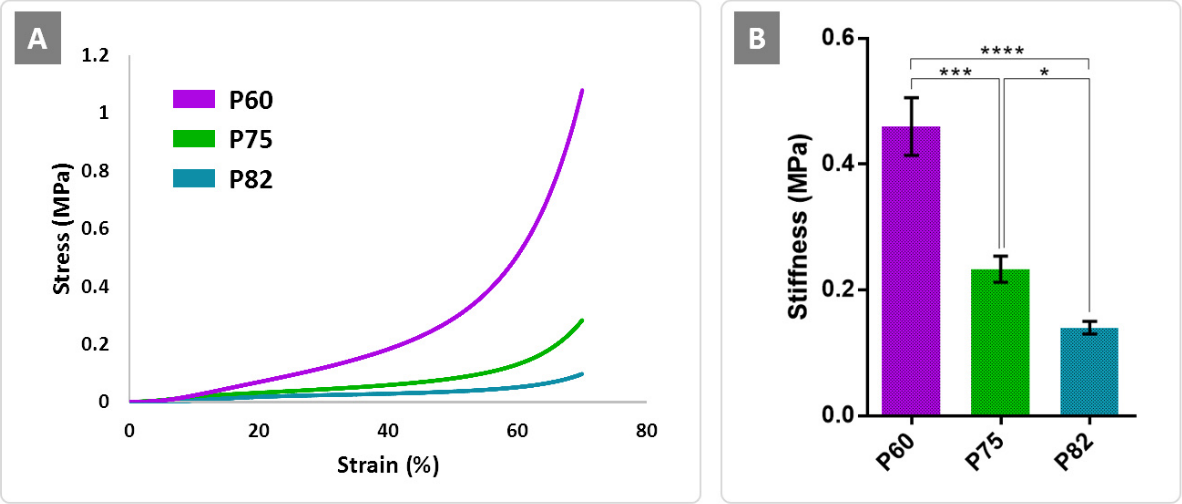

Fig. 6. **Compression test results. (A) Stress-strain curve and (B) stiffness of the polymerised emulsions prepared with varying internal phase volumes (n=3, ****P<0.0001, ***P<0.001, and *P<0.05).**

hind this result are likely to be the shrinkage of the polymer during polymerisation and drying and the variation of the degree of shrinkage depending on the thickness of the struts between neighbouring pores. Figs. 4A, 4D, and 4G show the zoom-out images of the full-thickness samples. No separated, non-porous polymer layer of any heterogeneous region was detected on the SEM images. In our previous study, we have shown that a full layer of non-porous polymer region appears in the SEM images of the polymerised unstable emulsions. This phase occurs on the bottom layer of the samples due to the density difference between the water and the oil phases [23, 35]. Accordingly, in this study, we can verify the stability of emulsions until the polymerisation point in light of SEM images.

No direct correlation between average pore size and internal phase volume was observed. In the SEM images of the P60 group, it can clearly be seen that water droplets are not crowdedly packed; there are distinguishable non-porous regions (shown with orange arrows). Increasing internal phase volume from 60% to 75% is likely to force water droplets to be more tightly packed with smaller-sized pores. Pore and window size distributions become broader in P82 when compared with P60 and P75 (Figs. 5A-5F).

There can be various potential reasons behind these observations. Firstly, as the internal phase is incorporated into the system dropwise, water droplets incorporated at the early stages are exposed to a longer duration of mechanical force to be divided and form smaller droplets, while the last portion of the internal phase is exposed to a shorter time of mixing and form larger droplets. Secondly, as internal phase volume increases, it leads to an increase in the emulsion viscosity, which may also have an adverse effect on the mixing efficiency and end up with broader pore size distribution. Thirdly, as there is enough continuous phase at the beginning, there is enough interfacial film that can form around the water droplets and let them increase their surface area by reducing their sizes [41]. Lastly, at the beginning of the emulsification, there is enough surfactant in the composition that can be placed around the water droplets to reduce the interfacial tension and eventually cause smaller pore size and increased emulsion stability. However, as the internal phase volume and the interfacial area increase, the surfactant amount falls short, the emulsion eventually results in larger pores, and the emulsion system does not accept a further increase in the internal phase volume. Barbetta *et al*. reported an increase in both pore and window diameters with increasing internal phase volume [41].

Both the average window sizes and the degree of interconnectivity values increase with increasing internal phase volume. This is potentially due to the enhanced packing density of the water droplets. As a result, the thickness of the interfacial polymer film between the pores is likely to reduce and more likely to rupture during polymerisation, resulting in the formation of interconnects [19].

In the stress-strain graph obtained from the compression test, it can be clearly seen that, at low strain, where stiffness values were calculated, stress-strain values were linear, and dramatic increases in stress were observed with increasing strain. In the stress-strain curve of porous polymers, as the compression load increases, the walls separating the pores are crushed, the porous material densifies, and the stiffness increases [29, 42]. Increasing internal phase volume from 60% to 82% caused a more than 2-fold reduction in the stiffness of the emulsion-templated matrices. If the pore and window sizes were the same for all three groups, this difference could be interpreted only because of the increasing porosity of the scaffolds. However, by increasing the internal phase volume, % porosity, pore size, window size and degree of interconnectivity values of the matrices are also changed. Thus, it can be concluded that the difference between the mechanical characteristics of these matrices is because of the cumulative effect of all of these changes. For instance, both window size and degree of interconnectivity values increase with increasing internal phase volume, which means the densities of the walls are less in scaffolds prepared with higher internal phase volumes, and this would cause a reduction in the stiffness of the designs.

Our group characterised the mechanical properties of a low degree of methacrylation (~50%) 4CPLMA-based PolyHIPEs prepared with different surfactant and solvent compositions previously [35, 43, 44]. Tensile modulus values were reported to be around ~0.4 MPa in these studies. Jackson *et al*. recently reported the compression modulus of 4PCLMA-based PolyHIPEs with a molecular weight of 20331 g/mol, methacrylation degree of 95%, and an average pore size of ~50 µm as ~1 MPa [39]. However, the compression behaviour of low molecular weight (with molecular weight ~2500 g/mol) 4PCLMA (with a high degree of methacrylation) PolyHIPEs are characterised for the first time in this study.

CONCLUSION

There is a wide range of characteristics of tissue engineering scaffolds that need to be engineered for specific biomedical applications. Mechanical characteristics and porosity are two of the important ones, alongside the pore size, window size, and interconnectivity. Although scaffolds with high porosity are desired to boost mass transfer and cell penetration throughout the scaffold, the stiffness of a scaffold is inversely proportional to porosity, as increased porosity simply reduces the solid portion of the scaffolds. In this study, we observed that average pore size and average window diameters can be increased by 30% and almost two-fold, respectively, simply by increasing the internal phase volume from 75% to 82%. However, the stiffness of the scaffolds also reduces almost twofold within these groups. To conclude, in this study, we established a relationship between internal phase volume and the physical, morphological and mechanical characteristics of 4PCMA-based emulsion templated scaffolds to be able to tune these characteristics for specific tissue engineering applications.

Authors' Contribution

Study Conception: BAD; Study Design: BAD; Supervision: BAD; Funding: BAD; Materials: BAD; Data Collection and/or Processing: BAD; Statistical Analysis and/or Data Interpretation: BAD; Literature Review: BAD; Manuscript Preparation: BAD and Critical Review: BAD.

Ethics Approval

There are no ethical issues with the publication of this manuscript.

Conflict of interest

The author disclosed no conflict of interest during the preparation or publication of this manuscript.

Funding

This study was supported by the Department of Scientific Research Projects of Izmir Institute of Technology (IZTECH-BAP, 2021-IYTE-1-0110 and 2022-IYTE-2-0025), Health Institutes of Turkey (TUSEB-2022B02-22517).

Acknowledgement

The author also acknowledges IzTech (Izmir Institute of Technology) Integrated Research Centers (IzTech IRC), the Center for Materials Research.

REFERENCES

1. Mert MS, Mert EH, Pulko I, Krajnc P, Mert HH. Form-stable oleic acid based polyHIPE/nanoclay framework supported composite phase change materials for low−temperature latent heat storage. Therm Sci Eng Prog. 2024;50(5):102569. doi: 10.1016/j.tsep.2024.102569.
2. Silverstein MS. PolyHIPEs: Recent advances in emulsion-templated porous polymers. Prog Polym Sci. 2014;39(1):199-234. doi: 10.1016/j.progpolymsci.2013.07.003.
3. Kovacic S, Schafzahl B, Matsko NB, et al. Carbon Foams via Ring-Opening Metathesis Polymerization of Emulsion Templates: A Facile Method to Make Carbon Current Collectors for Battery Applications. ACS Appl Energy Mater. 2022;5(11):14381-14390. doi: 10.1021/acsaem.2c02787.
4. Zowada R, Foudazi R. Macroporous hydrogels for soil water retention in arid and semi-arid regions. RSC Appl Polym. 2023;1(2):243-253. doi: 10.1039/d3lp00117b.
5. Kovacic JM, Ciringer T, Ambrozic-Dolinsek J, Kovacic S. Use of Emulsion-Templated, Highly Porous Polyelectrolytes for In Vitro Germination of Chickpea Embryos: a New Substrate for Soilless Cultivation. Biomacromolecules. 2022;23(8):3452-3457. doi: 10.1021/acs.biomac.2c00593.
6. Mert EH, Kaya MA, Yildirim H. Preparation and characterization of polyester-glycidyl methacrylate polyHIPE monoliths to use in heavy metal removal. Des Monomers Polym. 2012;15(2):113-126. doi: 10.1163/156855511X615001.
7. Aldemir Dikici B, Claeyssens F. Basic Principles of Emulsion Templating and Its Use as an Emerging Manufacturing Method of Tissue Engineering Scaffolds. Front Bioeng Biotechnol. 2020;8:875. doi: 10.3389/fbioe.2020.00875.
8. Sears NA, Dhavalikar PS, Cosgriff-Hernandez EM. Emulsion Inks for 3D Printing of High Porosity Materials. Macromol Rapid Commun. 2016;37(16):1369-1374. doi: 10.1002/marc.201600236.
9. Moglia R, Whitely M, Brooks M, Robinson J, Pishko M, Cosgriff-Hernandez E. Solvent-free fabrication of polyHIPE microspheres for controlled release of growth factors. Macromol Rapid Commun. 2014;35(14):1301-1305. doi: 10.1002/marc.201400145.
10. Christenson EM, Soofi W, Holm JL, Cameron NR, Mikos AG. Biodegradable Fumarate-Based PolyHIPEs as Tissue Engineering Scaffolds. Biomacromolecules. 2007;8(12):3806-3814. doi: 10.1021/bm7007235.
11. Knight E, Murray B, Carnachan R, Przyborski S. Alvetex®: polystyrene scaffold technology for routine three dimensional cell culture. Methods Mol Biol. 2011;695:323-340. doi: 10.1007/978-1-60761-984-0_20.
12. Aldemir Dikici B. Development of emulsion templated matrices and their use in tissue engineering applications. The University of Sheffield, PhD thesis; 2020. Available from: https://etheses.whiterose.ac.uk/27827/
13. Langer R, Vacanti JP. Tissue engineering. Science. 1993;260(5110):920-926. doi: 10.1126/science.8493529.
14. Dikici S. Enhancing wound regeneration potential of fibroblasts using ascorbic acid-loaded decellularized baby spinach leaves. Polym Bull. 2024;81:9995-10016. doi: 10.1007/s00289-024-05185-1.
15. Tamburaci S, Tihminlioglu F. Development of Si doped nano hydroxyapatite reinforced bilayer chitosan nanocomposite barrier membranes for guided bone regeneration. Mater Sci Eng C Mater Biol Appl. 2021;128:112298. doi: 10.1016/j.msec.2021.112298.
16. Pashneh-Tala S, Moorehead R, Claeyssens F. Hybrid manufacturing strategies for tissue engineering scaffolds using methacrylate functionalised poly(glycerol sebacate). J Biomater Appl. 2020;34(8):1114-1130. doi: 10.1177/0885328219898385.
17. Owen R, Sherborne C, Evans R, Reilly GC, Claeyssens F. Combined Porogen Leaching and Emulsion Templating to produce Bone Tissue Engineering Scaffolds. Int J Bioprint. 2020;6(2):265. doi: 10.18063/ijb.v6i2.265.
18. Aldemir Dikici B, Chen M-C, Dikici S, Chiu H-C, Claeyssens F. In Vivo Bone Regeneration Capacity of Multiscale Porous Polycaprolactone-Based High Internal Phase Emulsion (PolyHIPE) Scaffolds in a Rat Calvarial Defect Model. ACS Appl Mater Interfaces. 2023;15(23):27696-27705. doi: 10.1021/acsami.3c04362.
19. Cameron NR. High internal phase emulsion templating as a route to well-defined porous polymers. Polymer. 2005;46(5):1439-1449. doi: 10.1016/j.polymer.2004.11.097.
20. Silverstein MS. Emulsion-templated porous polymers: A retrospective perspective. Polymer. 2014;55(1):304-320. doi: 10.1016/j.polymer.2013.08.068.
21. Zhang T, Sanguramath RA, Israel S, Silverstein MS. Emulsion Templating: Porous Polymers and beyond. Macromolecules. 2019;52(15):5445-5479. doi: 10.1021/acs.macromol.8b02576.
22. Pulko I, Krajnc P. High internal phase emulsion templating - A path to hierarchically porous functional polymers. Macromol Rapid Commun. 2012;33(20):1731-1746. doi: 10.1002/marc.201200393.
23. Aldemir Dikici B, Dikici S, Claeyssens F. Synergistic effect of type and concentration of surfactant and diluting solvent on the morphology of highly porous emulsion templated tissue engineering scaffolds. React Funct Polymers. 2022;180(11):105387. doi: 10.1016/j.reactfunctpolym.2022.105387.
24. Dhavalikar P, Shenoi J, Salhadar K, et al. Engineering Toolbox for Systematic Design of PolyHIPE Architecture. Polymers (Basel). 2021;13(9):1479. doi: 10.3390/polym13091479.
25. Sengokmen-Ozsoz N, Boston R, Claeyssens F. Investigating the Potential of Electroless Nickel Plating for Fabricating Ultra-Porous Metal-Based Lattice Structures Using PolyHIPE Templates. ACS Appl Mater Interfaces. 2023;15(25):30769-30779. doi: 10.1021/acsami.3c04637.
26. Barbetta A, Cameron NR. Morphology and surface area of emulsion-derived (PolyHIPE) solid foams prepared with oil-phase soluble porogenic solvents: Span 80 as surfactant. Macromolecules. 2004;37(9):3188-3201. doi: 10.1021/ma0359436.
27. Durgut E, Sherborne C, Aldemir Dikici B, Reilly GC, Claeyssens F. Preparation of Interconnected Pickering Polymerized High Internal Phase Emulsions by Arrested Coalescence. Langmuir. 2022;38(36):10953-10962. doi: 10.1021/acs.langmuir.2c01243.
28. McKenzie TJ, Ayres N. Synthesis and Applications of Elastomeric Polymerized High Internal Phase Emulsions (PolyHIPEs). ACS Omega. 2023;8(23):20178-20195. doi: 10.1021/acsomega.3c01265.
29. Guarino V, Causa F, Ambrosio L. Porosity and mechanical

properties relationship in PCL porous scaffolds. J Appl Biomater Biomech. 2007;5(3):149-157. doi: 10.1177/228080000700500303.

30. Mert EH, Mert HH. Preparation of polyHIPE nanocomposites: Revealing the influence of experimental parameters with the help of experimental design approach. Polym Compos. 2021;42(2):724-738. doi: 10.1002/PC.25861.

31. Paterson TE, Gigliobianco G, Sherborne C, et al. Porous microspheres support mesenchymal progenitor cell ingrowth and stimulate angiogenesis. APL Bioeng. 2018;2(2):026103. doi: 10.1063/1.5008556.

32. Wang A, Paterson T, Owen R, et al. Photocurable high internal phase emulsions (HIPEs) containing hydroxyapatite for additive manufacture of tissue engineering scaffolds with multi-scale porosity. Mater Sci Eng C Mater Biol Appl. 2016;67:51-58. doi: 10.1016/j.msec.2016.04.087.

33. Owen R, Sherborne C, Paterson T, Green NH, Reilly GC, Claeyssens F. Emulsion templated scaffolds with tunable mechanical properties for bone tissue engineering. J Mech Behav Biomed Mater. 2016;54:159-172. doi: 10.1016/j.jmbbm.2015.09.019.

34. Woodruff MA, Hutmacher DW. The return of a forgotten polymer - Polycaprolactone in the 21st century. Prog Polym Sci (Oxford). 2010;35(10):1217-1256. doi: 10.1016/j.progpolymsci.2010.04.002.

35. Aldemir Dikici B, Sherborne C, Reilly GC, Claeyssens F. Emulsion templated scaffolds manufactured from photocurable polycaprolactone. Polymer (Guildf). 2019;175:243-254. doi: 10.1016/j.polymer.2019.05.023.

36. Aldemir Dikici B, Reilly GC, Claeyssens F. Boosting the Osteogenic and Angiogenic Performance of Multiscale Porous Polycaprolactone Scaffolds by In Vitro Generated Extracellular Matrix Decoration. ACS Appl Mater Interfaces. 2020;12(11):12510-12524. doi: 10.1021/acsami.9b23100.

37. Xu WF, Bai R, Zhang FA. Effects of internal-phase contents on porous polymers prepared by a high-internal-phase emulsion method. J Polym Res. 2014;21:524. doi: 10.1007/s10965-014-0524-2.

38. Karaca I, Aldemir Dikici B. Quantitative Evaluation of the Pore and Window Sizes of Tissue Engineering Scaffolds on Scanning Electron Microscope Images Using Deep Learning. ACS Omega. 2024;9(23):24695-24706. doi: 10.1021/acsomega.4c01234.

39. Jackson CE, Doyle I, Khan H, et al. Gelatin-containing porous polycaprolactone PolyHIPEs as substrates for 3D breast cancer cell culture and vascular infiltration. Front Bioeng Biotechnol. 2024;11:1321197. doi: 10.3389/fbioe.2023.1321197.

40. Kravchenko OG, Gedler G, Kravchenko SG, Feke DL, Manas-Zloczower I. Modeling compressive behavior of open-cell polymerized high internal phase emulsions: Effects of density and morphology. Soft Matter. 2018;14(9):1637-1646. doi: 10.1039/c7sm02043k.

41. Barbetta A, Dentini M, Zannoni EM, De Stefano ME. Tailoring the porosity and morphology of gelatin-methacrylate polyHIPE scaffolds for tissue engineering applications. Langmuir. 2005;21(26):12333-12341. doi: 10.1021/la0520233.

42. Hoque ME, San WY, Wei F, et al. Processing of polycaprolactone and polycaprolactone-based copolymers into 3D scaffolds, and their cellular responses. Tissue Eng Part A. 2009;15(10):3013-3024. doi: 10.1089/ten.TEA.2008.0355.

43. Aldemir Dikici B, Dikici S, Reilly GC, MacNeil S, Claeyssens F. A Novel Bilayer Polycaprolactone Membrane for Guided Bone Regeneration: Combining Electrospinning and Emulsion Templating. Materials (Basel). 2019;12(16):2643. doi: 10.3390/ma12162643.

44. Dikici S, Aldemir Dikici B, MacNeil S, Claeyssens F. Decellularised extracellular matrix decorated PCL PolyHIPE scaffolds for enhanced cellular activity, integration and angiogenesis. Biomater Sci. 2021;9(21):7297-7310. doi: 10.1039/d1bm01262b.